High-latitude crochet: solar flare-induced magnetic disturbance independent from low-latitude

Masatoshi Yamauchi[1], Magnar G. Johnsen[2], Carl-Fredrik Enell[3], Anders Tjulin[3], Anna Willer[4], and Dmitry A. Sormakov[5]

[1]Swedish Institute of Space Physics (IRF), Kiruna, Sweden
[2]Tromsø Geophysical Observatory (TGO), UiT the Arctic University of Norway, Tromsø, Norway
[3]EISCAT Scientific Association, Kiruna, Sweden
[4]National Space Institute, Technical University of Denmark (DTU Space), Kgs. Lyngby, Denmark
[5]Arctic and Antarctic Research Institute (AARI), St. Petersburg, Russia

Correspondence: M.Yamauchi (M.Yamauchi@irf.se)

Abstract. Solar flare-induced High latitude (peak at 70-75° geographic latitude) ionospheric current system was studied. Right after the X9.3 flare on 6 September 2017, magnetic stations at 68-77° geographic latitudes (GGlat) near local noon detected northward geomagnetic deviations (ΔB) for more than 3 hours, with peak amplitudes >200 nT, without any accompanying substorm activities. From its location, this solar flare effect, or crochet, is different from previously studied ones, namely,

5 subsolar crochet (seen at lower latitude), auroral crochet (pre-requires auroral electrojet in sunlight), or cusp crochet (seen only in the cusp). The new crochet is much more intense and longer in duration than the subsolar crochet. The long duration matches with the period of high solar X-ray flux (more than M3-class flare level). Unlike the cusp crochet, interplanetary magnetic field (IMF) B_Y is not the driver with B_Y only 0-1 nT out of 3 nT total field. The equivalent ionospheric current flows eastward in a limited latitude range but extended at least 8 hours in local time (LT), forming a zonal current region equatorward of the polar

10 cap on the geomagnetic closed region.

EISCAT radar measurements over the same region as the most intense ΔB near local noon show enhancements of electron density (and hence ion-neutral ratio) at these altitudes (100 km) where the background Sq ion convection (> 100 m/s) pre-existed. Therefore, this new zonal current can be related to the Sq convection and the electron density enhancement, e.g., by descending E-region height. However, we have not found why the new crochet is found in a limited latitudinal range, and

15 therefore the mechanism is still unclear compared to the subsolar crochet that is maintained by transient re-distribution of electron density.

The signature is sometimes seen in the Auroral Electrojet (AE) index. A quick eye-survey for X-class flares during solar cycle 23 and 24 shows clear AU increases for about half the >X2 flares during non-substorm time, although the latitudinal coverage of the AE stations is not favorable to detect this new crochet. Although some of them could be due to auroral crochet,

20 this new crochet can be rather common feature for X flares.

key points

(1) We found a new type of the solar flare effect on the dayside ionospheric current at high latitudes but equatorward of the cusp during quiet periods.

(2) The effect is also seen in the AU index for nearly half of the >X2-class solar flares.

25 (3) A case study suggests that the new crochet is related to the Sq current.

Copyright statement. TEXT

1 Introduction

Solar flares are known to enhance the ionospheric electron density and thus influence the electric currents in the D- and E-region. The geomagnetic disturbance (ΔH, ΔD, and ΔZ) caused by this current system is called a "crochet" or "SFE (solar

30 flare effect)" (e.g., Dodson and Hedeman, 1958). Crochets are observed at dayside low-latitudes with a peak near the subsolar region (Curto et al., 1994), in the nightside high-latitude auroral region with a peak where the geomagnetic disturbance ΔB pre-exists during solar illumination (Pudovkin and Sergeev, 1977) and in the cusp (Sergeev, 1977). This paper distinguishes them by calling them "subsolar crochet", "auroral crochet", and "cusp crochet", respectively.

The subsolar crochet is most likely caused by a re-distribution of the electron density at < 120 km altitude that is enhanced

35 by the flare X-ray (e.g., Curto et al., 1994; Yamasaki and Maute, 2017), resulting in a twin-vortex (one in each hemisphere) ionospheric current that is similar to the Sq (solar quiet) current. All recent studies of the crochet (it is simple called crochet without distinction) refer to this type of disturbance.

The auroral crochet is most likely caused by modification of a pre-existing ionospheric current (or electrojet) by the enhanced electron density (Pudovkin, 1974). This effect increases as background plasma convection (ionospheric electric field) increases,

40 and hence is most visible during the polar disturbances DP1 and DP2 (Akasofu, 1964; Nishida, 1968) as long as the ionosphere is sunlit, for example, near summer solstice when X-ray flux reaches high latitudes.

The preference of strong background plasma convection applies even to ΔB in the cusp that is strongly controlled by the interplanetary magnetic field (IMF) B_Y: DPY (Friis-Christensen and Wilhjelm, 1975; Levitin et al., 1982). DPY is associated with narrow convection "throat", which is deflected eastward or westward depending on the IMF B_Y polarity (Heelis et al.,

45 1976; Yamauchi and Slapak, 2018), and hence solar flare-induced ΔB at the cusp is expected to show strong IMF B_Y dependence during quiet periods. In fact, Sergeev (1977) showed one case each for both IMF polarities, showing that ΔB at > 80° latitude are in the same direction as IMF B_Y-dependent geomagnetic disturbances. This is the reason for calling this type of crochet "cusp crochet."

The amplitude and duration of the subsolar crochet is few tens nT and less than 30 min (mean 16-20 min) no matter how

50 long the high X-ray flux continues (Sergeev, 1977; Curto et al., 1994). Even after X9.3 flare on 6 September 2017, ΔB was only about 70 nT and it ended in less than 20 minutes (Curto et al., 2018), although the X-ray flux exceeded the X-flare level for nearly two hours (12:00-13:40 UT) as shown in Figure 1a. Thus, the subsolar crochet is a transient event that corresponds to the change in the global distribution of electron density after the solar flare but not maintained by high radiation flux.

The relevant ionospheric current is expected to be limited to low- and mid-latitude in the dayside, and the observed subsolar
crochet amplitude actually diminishes toward terminator and high latitudes. Therefore, the subsolar crochet near the terminator
has simply been assumed negligible, being driven by the weak return current of the crochet current (e.g., Annadurai et al.,
2018). With the resultant day-night asymmetric nature, the subsolar crochet can be detected as a short-lived (15-20 min) spike
in mid-latitude geomagnetic indices ASY-H and ASY-D (Singh et al., 2012), whereas the deviation is barely seen in high-
latitude indices AU and AL except near the summer solstice (Sergeev, 1977).

Compared to the subsolar crochet, crochets at high latitudes including the auroral crochet have not been much studied for 4
decades. This is partly because crochets at high latitudes during quiet periods were considered as the simple extension of the
subsolar crochets to the summer solstice, and partly because the purpose of the high-latitude crochet studies in the 1970's was
to understand the ionospheric electric field during disturbed periods. Such derivation requires many assumptions (Pudovkin and
Sergeev, 1977). Since the 1980's, more direct methods (satellite and radar measurements) than using geomagnetic signatures
took over for the E-field studies, which led to low research activity on crochets at high latitudes even during quiet times.

However, as shown in this paper, we found that the crochet at high latitudes is not a simple extension or sub-effect of, but
is independent from the subsolar crochet with larger amplitude and longer duration. We show this from a case study of X9.3
flare on 6 September 2017. We also show how these effect are seen in geomagnetic AE index using about 60 non-substorm
time flares of >X2 class during past two solar cycles (cycle 23 and 24). The solar flare X-ray data observed by GOES satellites
are obtained from NOAA, and the geomagnetic indices are obtained from the world data center (Kyoto and Copenhagen). The
other data are described in Yamauchi et al. (2018).

2 High-latitude crochet for X9.3 flare on 6 September, 2017

In the overview paper of EISCAT radar observations and geomagnetic disturbances near local noon during the 6-8 September
2017 space weather event, Yamauchi et al. (2018) briefly mentioned a sudden enhancement of ΔB (> 150 nT) at high latitudes
(> 68° GGlat) in response to the X9.3 flare on 6 September, 2017, but without special note nor detailed description on this
high-latitude disturbance compared to subsolar crochets, auroral crochets, or cusp crochets.

2.1 Subsolar crochet after X9.3 flare

Figure 1b shows detailed time profiles of the northern Scandinavian magnetograms at >65° GGlat, which are located near local
noon when the X9.3 flare took place. IMF was weak with total field less than 3 nT (B_X = -1 nT, B_Y = 1 to 0 nT, B_Z = -2 nT
during 12:00-13:00 UT in Geocentric Solar Magnetospheric coordinate), and the geomagnetic indices (Figure 2) indicate that
the X9.3 flare started after the end of dayside activity related to the previous substorm, without magnetic storm activity. The
IMF B_Y condition indicates that the cusp crochet must be small or invisible.

The subsolar crochet was observed as the short-lived geomagnetic deviation starting nearly simultaneously as the increase
of X-ray flux at the Earth and lasted about 10-15 minutes at Sørøya (SOR, 70.5° GGlat), Tromsø (TRO, 69.7° GGlat), Kiruna
(KIR, 67.8° GGlat), Rørvik (RVK, 65.0° GGlat.). All equatorward stations show the same type of disturbances (Curto et al.,
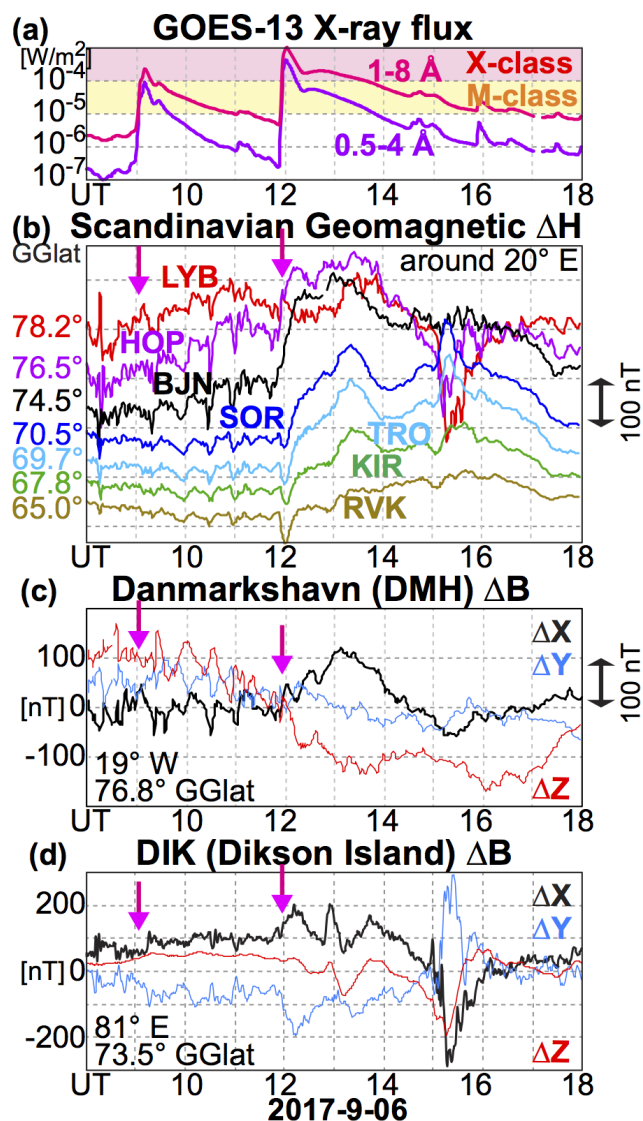
Figure 1. (a) Solar X-ray flux. (b) Stack-plot of geomagnetic H component for Kiruna (KIR) and northern Norway. (c) Geomagnetic data at Danmarkshavn (DMH) and (d) at Dikson Island (DIK).

2018). This is also seen in ASY-D (63 nT at 12:04 UT) and ASY-H (77 nT at 12:05 UT) as shown in Figure 2a, with amplitude change by the flare about 60 nT. One can even recognize a crochet-like signature in ASY-D when an X2.2 flare occurred at around 9:00 UT.
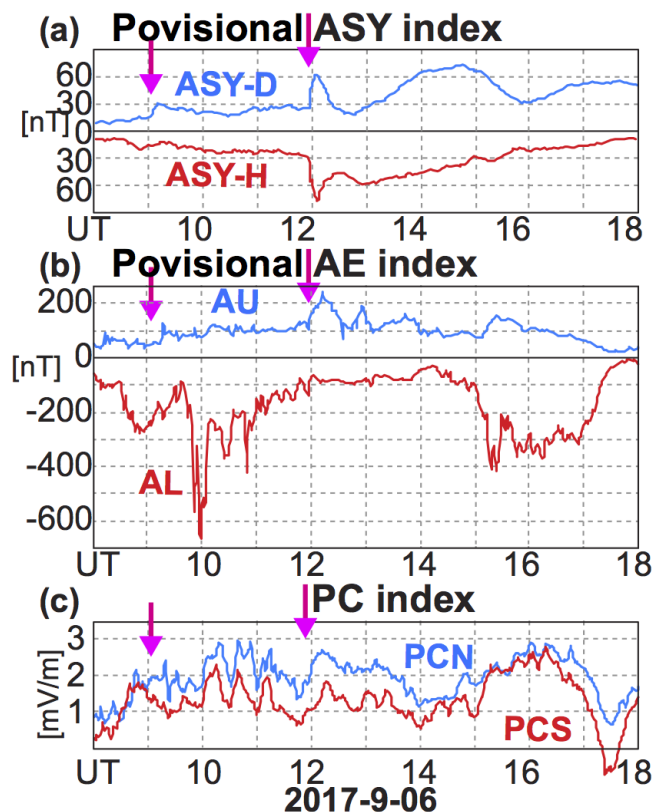
Figure 2. Geomagnetic ASY, AE, PC indices.

2.2 New crochet after X9.3 flare

The new finding is the subsequent geomagnetic disturbances: a large positive ΔH deviation (northward ΔB) also started right after or even during the negative ΔH spike (south-weastward ΔB) of the subsolar crochet, with much higher amplitudes as shown in Figure 1b. This positive ΔH continued for hours with the peak at around 13:00 UT at Bear Island (BJN) at 74.5° GGLat (> 200 nT), 13:20 UT at 70° GGlat (SOR and TRO: 180 nT) and 68° GGlat (KIR: 140 nT), and 14:50 UT at 65° GGlat (ROR: 70 nT). With larger amplitude and longer duration than the subsolar crochet, this geomagnetic signature is visible even in the AU index, as shown in Figure 2b, although the baseline is as large as 100 nT due to the previous substorm activity and can hide the subsolar crochet if any exists.

The development is also quick. At BJN (74.5° GGlat), ΔH reached $\Delta H>65$ nT at already 12:05 UT, i.e., at the peak time of the subsolar crochet, and reached 130 nT at already 12:20 UT. Since the long duration already indicates that the generation mechanism is different from that of the subsolar crochet (re-distribution of electron), the positive ΔH of this crochet with diminishing amplitude toward lower latitude should cancel the negative ΔH of the subsolar crochet at high-latitude. In fact, ΔH exceeded the value before the flare at 12:10 UT at 70° GGlat, 12:12 UT at 68° GGlat, and 12:17 UT at 65° GGlat.

These large ΔH, however, is observed in a limited latitudinal range, diminishing toward higher latitudes with 140 nT at 76.5° GGlat (Hopen: HOP, at 12:50 UT) and not visible at 78.2° GGlat (Longyearbyn: LYB). Since the geomagnetic latitude of LYB is only 75.3° and IMF is weak with $B_Y = 0$ nT, the positive ΔH is limited to the geomagnetic closed region outside

105   the cusp nor polar cap. The closed geometry is also indicated by the EISCAT Svalbard radar data (Yamauchi et al., 2018). The PC index (Polar Cap index), which corresponds to the polar cap activity, shows enhanced values in the same period, but not as prominent as in AU, as shown in Figure 2.

On the other hand, positive ΔB at around 75° GGlat was observed in a wide local time range, as shown in Figures 1c and 1d (ΔX is nearly the same as ΔH in both stations). Danmarkshavn (DMH) at 19°W and Dikson Island (DIK) at 81°E showed ΔX

110   about 120 nT and 100 nT from before the flare at around 13:00 UT, respectively. Together with the zero IMF B_Y condition, the observed large ΔH cannot be a cusp crochet. Considering its location and pre-existing activity, this crochet is neither the subsolar crochet nor auroral crochet, although some part of the observed ΔH could be affected by the auroral crochet.

For example, DIK is located near the evening terminator (it is still under sunlight near horizon) and the geomagnetic activity before 12 UT indicates some auroral activity. Therefore the first peak at around 12:20 UT, which is larger than that of BJN

115   or HOP and with more westward ΔB, can be the auroral crochet rather than the extension of the new crochet. However, the second and third peaks are in the same direction (northward ΔB) as near local noon, and multiple peaks are not expected for an auroral crochet does not under smoothly declining X-ray flux. Therefore, positive ΔX at DIK at around 13:00 UT and 13:40 UT can be interpreted as a part of the new high-latitude crochet rather than the auroral crochet, although we cannot dismiss the possibility of the auroral crochet.

120   With such large amplitude, the crochet is visible even in AU although the AU stations are not located at favorable GGlat. During 12:00-14:00 UT, AU has three positive peaks (provisional values of 240 nT at 12:12 UT, 190 nT at 12:55 UT, and 160 nT at 13:43 UT but further baseline subtraction might be needed). The timing of these peaks corresponds to the subsolar crochet and the high-latitude one at BJN, but the provisional AU value reflects DIK data (DIK is one of the AE station) as shown in Figures 1c and 2b. Although the amplitude is larger at BJN than DIK for the second and third peaks, BJN is located

125   far poleward of the AE stations and does not contribute to AU.

2.3   Equivalent ionospheric current

From the Norwegian and Greenland magnetometer data, we also calculated the ionospheric equivalent currents, using the Spherical Elementary Current System (SECS) technique (Amm, 1998; Amm and Viljanen, 1999). Here we obtained epsilon = 0.037 in a similar fashion as by Wygant et al (2012). The results are shown in Figures 3 and 4. Figure 3 shows latitudinal

130   distribution of the eastward current density crossing two meridians (Scandinavia: 20°E, and Greenland: 50°W) where actual magnetometer network deployed.

In Figure 3, one can see a sudden appearance in the ionospheric current in a wide region at around 12:00 UT when the X-ray flux from the X9.3 flare increased at the Earth. The enhancement is westward at lower latitudes (< 70° GGlat at 20°E or 13 LT, and <72°W at 50°W or 9 LT), and eastward at higher latitudes in the both meridians. They correspond to the

135   subsolar crochet current in the northern hemisphere (Curto et al., 2018) and the new high-latitude crochet mentioned above,
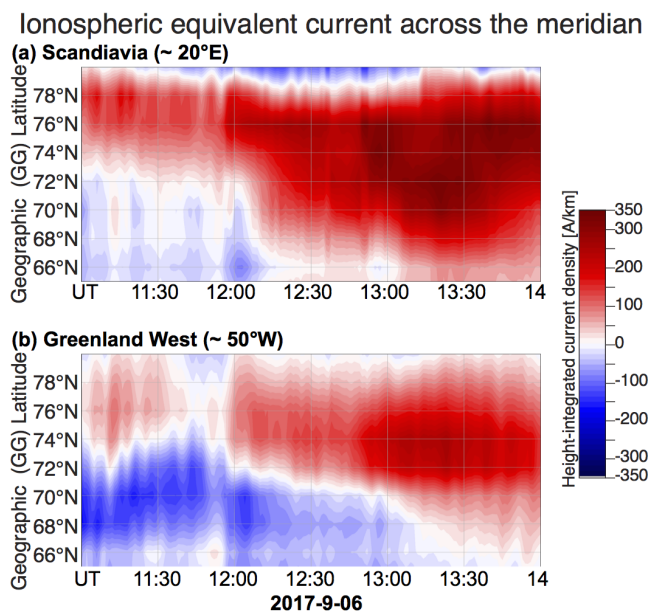
Figure 3. Latitudinal distribution of ionospheric equivalent current Eastward component crossing (a) Scandinavian meridian (20°E) and (b) Greenland meridian (50°W), based densely distributed magnetometer network. The Spherical Elementary Current System (SECS) technique is used. Data is displayed in a latitude-time spectrogram form over 11:00-14:00 UT, 6 September 2017, i.e., around the X9.3 flare.

respectively. Figures 4a and 4b show the 2D vector directions, corresponding to this timing: right before the flare (11:50 UT), at the subsolar crochet peak (12:04 UT). The low-latitude side composes the counter-clockwise current that agrees with the high-latitude return current direction of the subsolar crochet (Curto et al., 2018; Annadurai et al., 2018). The high-latitude side forms another independent counter-clockwise current, with strong eastward current near BJN(c. Figure 1) as mentioned above.

140   The resultant shear poleward of BJN corresponds to upward field-aligned current, i.e., afternoon Region 1 field-aligned current.

The eastward current expanded quickly in both longitudinal direction and toward lower latitude as soon as the subsolar crochet diminished. At the same time, the current density gradually increased toward its peak. Figures 4c and 4d show the 2D vector directions at these peaks: at the first minor peak of ΔH at around $75°$ GGlat (12:20 UT) after the subsolar crochet disappeared, and at the major peak of ΔH at around $70°$ GGlat (13:20 UT), respectively. By 12:20, region is this westward

145   current with peak at around 72-$74°$ GGlat expanded in a wide local time from Greenland to eventually Siberia (DIK at $81°$E as shown in Figure 1d), i.e., more than $130°$ in longitude. The entire current lies on the geomagnetic closed region as mentioned above, and its peak latitude gradually moved equatorward. By the peak time at around 13:20 UT, all region over $5°$ in latitude and $>100°$ in longitude are intensified, with much higher intensity than the subsolar crochet current.

The current direction of eastward (or positive ΔH) is the same as the ionospheric current in the evening auroral oval (we here

150   mean that the region between the upward region 1 field-aligned current and downward region 2 field-aligned current (Iijima and Potemra, 1976; Akasofu, 1977; Yamauchi and Slapak, 2018)), and the observed eastward current continued until the next substorm onset took place at 15:00 UT (cf. Figure 2b). However, no outstanding substorm is visible in AE (Figure 2b) or

DIK data (Figure 1c) before this substorm with continued weak IMF condition. The eastward current patch is even started at
Greenland meridian at 9 LT and continued toward the afternoon sector although IMF $B_Y = 0$ nT. Since there was no auroral

155 current signature at BJN before this crochet, this current system is not the auroral crochet current. Rather the question is how
much does this new crochet contribute to ΔB in the evening sector, including the auroral crochet. In this sense, we cannot
judge moment if the crochet detected in DIK is the evening extension of this crochet or auroral crochet or both effects mixed.

2.4 EISCAT data

For this X9.3 flare event on 6 September 2017, the duration of this new crochet matches with that of high X-ray flux: it was

160 at the X-class level until 13:40 UT and M-class level until 17 UT, as shown in Figure 1. From this coincidence, Yamauchi
et al. (2018) speculated the possibility of enhancement of pre-existing Sq (solar quiet) current without showing detailed data.
However, the Sq is driven by daily neutral convection starting from subsolar region, and hence it has long been expected to be
small at high-latitude (Yamasaki and Maute, 2017). Therefore, we need direct evidence with the Sq scenario. For that purpose,
Figures 5 shows ionospheric electron density and ion velocity, respectively, observed by EISCAT VHF radar at Tromsø.

165 Figure 5b shows that the electron densities in the 100-200 km altitude range were significantly enhanced by the enhanced
X-ray flux, starting at around 12 UT (doubling at 100 km altitude and seen up to 200 km altitude). Figure 5a shows that
northward ion convection was also enhanced, and more importantly that background Sq ions convection starting from around
9 UT is already strongly northward (away from the sub-solar region) with large values as much as 150 m/s at 71° Mlat (at 100
km altitude).

170 Since the increase in the electron density means also the increase of the ion-neutral density ratio, the altitude of ionospheric
current, is expected to decrease, reaching close to the altitude where the Sq convection is strong. Such changes can enhance
the pre-existing Sq current significantly, although this scenario does not easily explain why it is found in a limited latitudinal
range and wide longitude.

  The time development of the electron density enhancement together with the elevated ion velocity at 100 km matches with

175 the ΔH time profile at BJN that is located under the area observed by the EISCAT VHF radar. Note that ion velocity direction
(northward) is the electric field direction at this altitude where only ions are collisional with neutrals but not electrons, and hence
collision-free electrons drift westward, resulting in eastward an Hall current (that causes $\Delta H > 0$ geomagnetic disturbance).

  The EISCAT data in Figure 5d also revealed a decrease of electron density above 300 km after 12 UT. Since photochemistry
predicts density increase at all altitudes, this density decrease must be caused by ionospheric dynamics, such as 3D distribution

180 of ionospheric current, while this decrease does not affect the total current because the ion velocity at > 300 km is not changing
very much compared to the ion velocity at < 200 km, and not contributing to the ionospheric current.

3 Preliminary survey results

We further conducted quick survey of geomagnetic AXY/AE indices (cf. Figures 3a and 3b) during past two solar cycles. There
are 73 flare events with >X2 class since 1996. For all these events, we examined web-interfaced quick plot for AE and ASY,

Table 1. Survey of 73 flare events with >X2 class

signature	yes (@onset)[1]	unclear	no	(substorm)[2]	total
in ASY	52 (+5)	6	5	5	73
in AU	20 (+5)	7	30	11	73
in AL	11 (+5)	9	38	10	73

*1: Simultaneous with onset *2: Too disturbed to see the signature

by adding marks that indicate the X-ray flux level and start timing, as shown in Figure 6 for 15 July, 2002 event. We here show raw plot that is also found as the supplemental materials.

Table 1 shows the survey result. There are about 10 events are during substorms and difficult to judge if the variation is due to the flare or not. Among the remaining 63 cases, crochets are detected in ASY almost always, and the exceptions (5 cases) might be attributed to non-favorable distribution of ASY stations in terms of local time and GGlat at the time of flare (UT and season). Since auroral crochets and cusp crochets do not contribute to ASY, they are interpreted as subsolar crochets. In addition, crochets are detected in AU and AL for a substantial part of the cases. From the latitude of AE stations, they are either auroral

For auroral crochets, the precondition requirement is severe: a substantial auroral electrojet must pre-exist in the sunlit hemisphere. This removes more than half the cases, and therefore we expect that the new high-latitude crochet can also be observed in the AE index, as seen in Figure 3b and Figure 6. In Figure 6, even AL deviation started simultaneously as the crochet. Then the question is if this AL signature is related to the crochet or not. In this example, an X3.0 flare took place around 19:59 UT, with X-ray flux reaching M3-class flare level at around 20:05 UT and solar wind condition was stable with stable IMF. AE and ASY show a quiet condition before the flare, and all components (AU, AL, ASY-D, and ASY-H) showed sudden changes at 20:04 UT. The signature is not short-lived that is typical to the subsolar crochet.

To examine it further, Figure 7 shows the Scandinavian and Green land geomagnetic data at the same stations as Figure 1. We also added Kullorsuaq (KUV) data from the west coast of Greenland that is 18 MLT at the time of crochet.

Figure 7 shows sudden increase of ΔH at around 20:04 UT at all stations. In addition, negative spike started 20:07 UT at BJN, 20:13 UT at SOR, and at 20:15 UT at TRO. Except the duration, $\Delta H>0$ enhancement at high latitude is similar to what we observed in the 6 September 2017 event (Figure 1). The short duration is not surprising considering the high solar Zenith angle (it was about 63° in the Greenland). Since KUV's local time is only 17 LT, which is within the zonal extend of crochet according to DIK's data in the 6 September 2017 event (Figure 1), this $\Delta H>0$ is quite likely to be the new high-latitude crochet. Then the new high-latitude crochet extends toward the evening quite wide near the summer solstice. Even DIK data (which is 01 LT past the midnight but still under sunlight) showed minor signature. This suggest that AU signature is most likely caused by this crochet rather than auroral crochet.

On the other hand, unique bipolar signature with short-live $\Delta H>0$ is seen at BJN. This is a candidate for the auroral crochet. In addition, $\Delta B>0$ at SOR, TRO, and DIK can be read as the disruption of the substorm-related large magnetic bay. In fact,

a signature of small auroral electrojet is seen at BJN, SOR, TRO, and DIK before the crochet (starting at around 19:40 UT). Although the signature is not visible at Kiruna and the value at BJN returned normal, weak aurora existed in this narrow region before the crochet.

215   However, the auroral electric field before the crochet must be very weak compared to what was reported as the auroral crochet (Pudovkin and Sergeev, 1977), and at least the $\Delta H>0$ signature, that is consistently observed at many stations with quiet pre-condition, is better interpreted as the new crochet. Then we can even wonder if the interaction between the new crochet and the auroral oval accelerated the large $\Delta B<0$ bay.

3.1   Discussion and future tasks

220 ### 3.2   Why not found in the past?

Although magnetic stations have been extended toward higher latitudes beyond 68° GGlat since 1980's, this new crochet has never been reported, at least not to our knowledge. One possible reason is that the phenomenon is limited to a relatively small range in geographic latitude (68°-75° GGlat) while the station should be completely outside the geomagnetic cusp (< 75° Mlat). This criterion excludes many geomagnetic stations over Greenland and Canada from finding the new crochet.

225 ## 4   Need solid statistics and global perspective

Although we made a survey using quick plots, we need to make more solid analyses. For example, we need to include amplitudes (we examined only yes or no), examine the closure of the ionospheric current system at high latitudes, analyze global magnetometer network data, and take such statistics. Such a global perspective would also tell for which conditions the effect can be detected in AU or AL.

230   One important note is that the difference between the GGlat and Mlat (i.e., UT dependence) must be considered. Also, we have to note that the current system might be different between different events (size of flare may affect the intensity and size, season may affect the distribution pattern). In addition, if intensification of the Sq current is important, the new crochet might be the equinox phenomenon (Yamasaki and Maute, 2017). Therefore, it might be difficult to obtain consistent results, but at least a common feature can be obtained.

235 ### 4.1   What is the main driver of the new crochet?

As shown in Figure 4, this current system might be related to enhancement of the Sq current through the enhancement of both the ion/electron density and ion velocity (Pederson electric field). Then the question is the relative importance of these mechanisms. In addition, we need to understand the relation to the nightside crochet that we found a substantial number, but we have not even found the criterion how to classify the observed crochet as the auroral crochet or nightside extension of the

240 new crochet. To answer this, we need similar radar data for different events. Since the availability of radar data in favorable observation modes and geometry is limited (such as the investigated EISCAT data), we need other radar data including future

facility such as EISCAT 3D for a solid answer. Such a work also probably give some hints why the electron density decreased at > 300 km in Figure 4. Future satellite missions that cover ionospheric E-region, such as Daedalus (Sarris, et al., 2020), are strongly needed.

4.2   Can crochet trigger a substorm or M-I coupling?

In the preliminary survey, we found many "coincidence" cases in which large gradient of ΔH occurred at the same time as substorm onsets or sudden intensifications of substorms when X-flares took place. Figure 8 shows one such example when X6.2 flare took place at 19:13 UT, and substorm onset took place immediately after. Solar wind density and velocity were stable after CME arrival 7 hours before, and traditional explanation of the trigger is IMF changes.

However, the crochet mechanism can trigger a substorm through sudden intensification of ionospheric density and electric field through magnetosphere-ionosphere (MI) coupling (e.g., Kan et al., 1988). Furthermore, this substorm is peculiar with larger AU than AL right after the onset, in agreement with crochet whereas substorm onset is characterized large negative ΔH and AL. Since several different onset mechanism may causes the substorm, it is quite possible that crochet may also trigger a substorms, as one of minor onset mechanisms (Yamauchi, 2019). The investigation of such a scenario is a future task.

The same question arises with respect to the Magnetosphere-Ionosphere (M-I) coupling. The latitude range of the new crochet is inside the closed field-line region (near local noon), but yet close to the dayside Region 1 field-aligned current (Iijima and Potemra, 1976; Yamauchi and Slapak, 2018). This means that the new crochet might influence the field-aligned current system. Such a study requires satellite observation at right location and right timing.

4.3   Modulation of Pc5?

If the long lasting high X-ray flux influences the ionospheric current, some effect might arise from the X2.2 flare at 9 UT on the same day. One possibility is the density moderation synchronizing with the Pc5 pulsation during the recovery phase of the substorm that started at 09:37 UT with peak at 05:58 UT with AL=-666 nT (Figure 2). In fact, ΔH showed large-amplitude oscillations with periodicity about 30 min during 09:30-11:20 UT (Figure 1b). However, electron density at 150-200 km altitude showed irregular oscillations with a different periodicity (15 min) although no mediation is seen at 100 km altitude. The periodicity in the ion convection is also about 15 min for 150-200 km altitude. The only candidate that may match with 30 min periodicity is irregularity in the ion velocity at 100 km, but profile does not really match with the ΔH variation. This suggests that the Pc5 pulsation can be modulated by the density variation at 150-200 km altitude.

4.4   Relation to space weather

In addition to opening up new science case that is concentrated on 68-75° GGlat, large extra ΔH by X-ray during substorms might have some connection with space weather researches. Therefore, although this work is not currently related to any other researches, this has potential that may collaborate with other researches.

5 Conclusions

Using the Norwegian geomagnetic chain and EISCAT data, we found a new type of solar flare effect on the geomagnetic disturbance (SFE, or crochet) in response to the X9.3 flare on 6 September 2017 at high latitudes (65-75° GGlat). The new

275 crochet is found over a wide local time range including local noon but outside the cusp, i.e., in the geomagnetic closed region. It lasted for a longer duration with higher peak amplitude than the subsolar crochet. The equivalent ionospheric current flows eastward in a limited latitude range but extended at least 8 hours in local time (LT), forming a zonal current region at around 70-75° Geographic latitude (equatorward of the polar cap in at least in dayside). Considering its location and duration, this crochet is different from previously studied crochets (subsolar, auroral, and cusp).

280 Ionospheric parameters at local noon during this crochet shows strong background ion convection before the crochet as well as sharp enhancement of electron density (and hence the ion-neutral density ratio). Thus the new crochet can be related to increase electron density at 100-150 km altitudes, where strong Sq ion convection exists. For example, change in the E-layer height can actually cause the ionospheric current at high-latitude, but such scenario does not easily explain why it is found in a limited latitudinal range, and therefore the mechanism is still unclear.

285 We also examined the crochet signatures in AE and ASY indices for all X flares (> X2.0) over past two solar cycles. While the subsolar crochet is well recognized in ASY indices, crochet signatures that represent the new crochet or auroral crochet are also recognized in AU for half the cases, and even in AL index sometimes. However, AE alone cannot distinguish between this new crochet and the auroral crochet in the evening sector, and further studies is needed to understand the current system related to these crochets.

290 *Data availability.* The X-flare list is obtained from National Oceanic and Atmospheric Administration Space Weather Prediction Center (NOAA/SWPC) at

https://www.ngdc.noaa.gov/stp/solar/solarflares.html

and the X-ray data during these flare are obtained from

https://www.ngdc.noaa.gov/stp/satellite/goes/dataaccess.html

295 through plot at

https://www.polarlicht-vorhersage.de/goes-archive

that is created by Andreas Møller. AE and ASY indices (both ASCII data and web-interfaced plots) are obtained from World Data Center for Geomagnetism (WDC Kyoto) at

http://wdc.kugi.kyoto-u.ac.jp/aeasy/index.html

300 Geomagnetic data are available through Tromsø Geophysical Observatory (TGO) site, SuperMAG site, and IRF site

https://flux.phys.uit.no/geomag.html

http://supermag.jhuapl.edu/mag/?fideli

http://www2.irf.se/maggraphs/iaga/

The EISCAT common programme data is available at:

305 https://www.eiscat.se/madrigal/.

Author contributions. MY (first author) made all contribution. MJ provided Norwegian data and made Figures 3 and 4, and relevant interpretation. CE and AT calibrated EISCAT data and its interpretation. AW provided Greenland data and its interpretation. DS provided Diikson Island data and its interpretation. All contributed in constructing the argument that the phenomena is new.

Competing interests. no competing interests are present

310 *Acknowledgements.* We thank WDC kyoto, NOAA/SWPC, and SuperMAG for processed dataset. MY thanks Masahiko Takeda for general information on Sq.

References

Akasofu S.-I.: Physics of magnetospheric substorms, 619pp, ASSL v47, Reidel, 1977.

Amm, O.: Method of characteristics in spherical geometry applied to a Harang discontinuity situation, Ann. Geophys., 16, 413-424, doi:10.1007/s00585-998-0413-2, 1998.

Amm, O., and Viljanen, A.: Ionospheric disturbance magnetic field continuation from the ground to the ionosphere using spherical elementary currents systems, Earth Planets Space, 51, 431-440, doi:10.1186/BF03352247, 1999.

Annadurai, N.M.N., Hamid, N.S.A., Yamazaki, Y., and Yoshikawa, A.: Investigation of unusual solar flare effect on the global ionospheric current system, J. Geophys. Res.,, 123, 8599-8609, https://doi.org/10.1029/2018JA025601, 2018.

Curto, J.J., Amory-Mazaudier, C., Torta, J.M., and Menvielle, M.: Solar flare effects at Ebre: Regular and reversed solar flare effects, statistical analysis (1953 to 1985): A global case study and a model of elliptical ionospheric currents, J. Geophys. Res., 99, 3945-3954, doi:10.1029/93JA02270, 1994.

Curto, J.J., Marsal, S., Blanch, E., and Altadill, D.: Analysis of the solar flare effects of 6 September 2017 in the ionosphere and in the Earth's magnetic field using spherical elementary current systems, Space Weather, 16, 1709-1720. https://doi.org/10.1029/2018SW001927, 2018.

Curto, J.J., Juan, J., and Timote, C.: Confirming geomagnetic SFE by means of a solar flare detector based on GNSS. J. Space Weather Space Climate, 9, 1-15, doi:10.1051/swsc/2019040, 2019.

Dodson, H.W., and Hedeman, E.R.: Crochet-associated flares, Astrophys. J., 128, 636-645, 1958.

Heelis, R.A., Hanson, W.B., and Burch, J.L.: Ion convection velocity reversals in the dayside cleft, J. Geophys. Res., 81, 3803-3809, doi:10.1029/JA081i022p03803, 1976.

Iijima, T., and Potemra, T. A.: The amplitude distribution of field-aligned currents at northern high latitudes observed by Triad, J. Geophys. Res., 81, 2165, https://doi.org/10.1029/JA081i013p02165, 1976

Kan, J.R., Zhu, L., and Akasofu, S.-I.: A theory of substorms: Onset and subsidence, J. Geophys. Res., 93, 562-5640, https://doi.org/10.1029/JA093iA06p05624, 1988.

Ohtani, S., Gjerloev, J.W., Johnsen, M.G., Yamauchi, M., Brändström, U., and Lewis, A.M. : Solar illumination dependence of the auroral electrojet intensity: Interplay between the solar zenith angle and dipole tilt, J. Geophys. Res., 124, 6636-6653, https://doi.org/10.1029/2019JA026707, 2019.

Sarris, T. E., Talaat, E. R., Palmroth, M., Dandouras, I., Armandillo, E., Kervalishvili, G., Buchert, S., Tourgaidis, S., Malaspina, D. M., Jaynes, A. N., Paschalidis, N., Sample, J., Halekas, J., Doornbos, E., Lappas, V., Moretto Jørgensen, T., Stolle, C., Clilverd, M., Wu, Q., Sandberg, I., Pirnaris, P., and Aikio, A.: Daedalus: a low-flying spacecraft for in situ exploration of the lower thermosphere-ionosphere, Geoscientific Instrumentation, Methods and Data Systems, 9, 153-191, doi:10.5194/gi-9-153-2020, 2020.

Pudovkin, M.I.: Electric fields and currents in the ionosphere, Space Sci. Rev., 16, 727-770, doi:10.1007/BF00182599, 1974.

Pudovkin, M.I., and Sergeyev, V.: Magnetic effect -II-, Geomagnetizm i Aeronomiya - GEOMAGN AERON, 17, 496-501 (English translated vergion 336-339), 1977.

Sergeyev, V.: Magnetic effect -I-, Geomagnetizm i Aeronomiya - GEOMAGN AERON, 17, 291-297 (English translated vergion 194-198), 1977.

Singh, A.K., Sinha, A.K., Pathan, B.M., Rawat, R.: Solar flare effect on low latitude asymmetric indices, J. Atmos. Solar-Terrestr. Phys., 77, 119-124, https://doi.org/10.1016/j.jastp.2011.12.010, 2012.

Weygand, J. M., Amm, O., Viljanen, A., Angelopoulos, V., Murr, D., Engebretson, M. J., Gleisner, H., and Mann, I.: Application and validation of the spherical elementary currents systems technique for deriving ionospheric equivalent currents with the North American and Greenland ground magnetometer arrays, J. Geophys. Res., 116, A03305, doi:10.1029/2010JA016177, 2011.

Yamazaki, Y., and Maute, A.: Sq and EEJ-A review on the daily variation of the geomagnetic field caused by ionospheric dynamo currents, Space Sci. Rev., 206, 299-405, doi:10.1007/s11214-016-0282-z, 2017.

Yamauchi, M., Iyemori, T., Frey, H., and Henderson, M.: Unusually quick development of a 4000 nT substorm during the initial 10 min of the 29 October 2003 magnetic storm, J. Geophys. Res., 111, A04217, doi:10.1029/2005JA011285, 2006.

Yamauchi, M., Sergienko, T., Enell, C.-F., Schillings, A., Slapak, R., Johnsen, M. G., Tjulin, A., and Nilsson, H.: Ionospheric response observed by EISCAT during the September 6-8, 2017, space weather event: overview, Space Weather, 16, 1437-1450, doi:10.1029/2018SW001937, 2018.

Yamauchi, M.: Terrestrial ion escape and relevant circulation in space, Ann. Geophys., 37, 1197-1222, doi:10.5194/angeo-37-1197-2019, 2019.

350

355
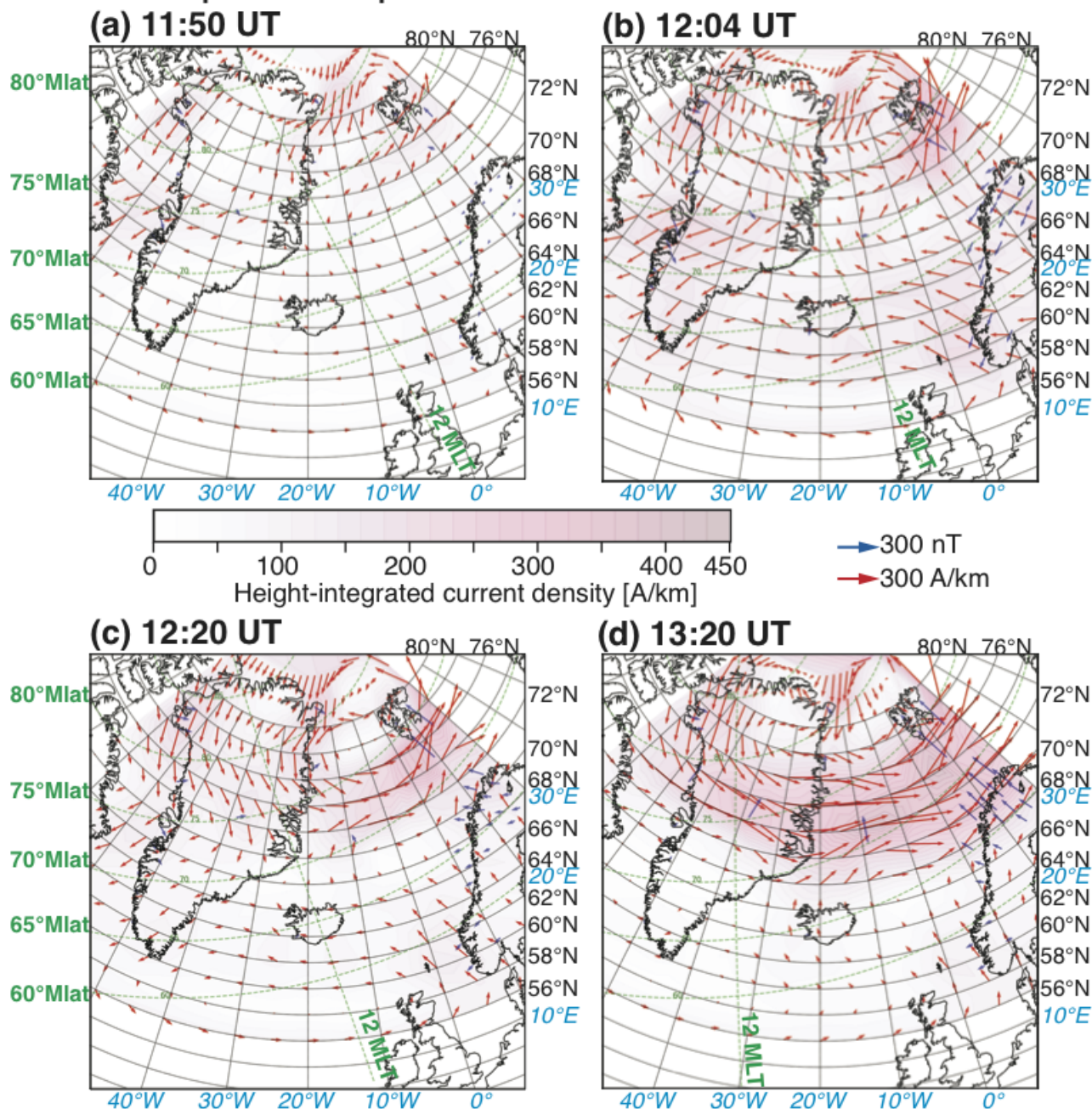
Figure 4. Ionospheric equivalent currents on 6 September 2017 based on Norwegian and Greenland magnetometers, using the same method as Figure 3. (a) Before the flare (11:50 UT), (b) the subsolar crochet peak (12:04 UT), (c) around the first peak at HOP and BJN (12:20 UT), (d) the main peak at SOR, TRO, and KIR (13:20 UT).
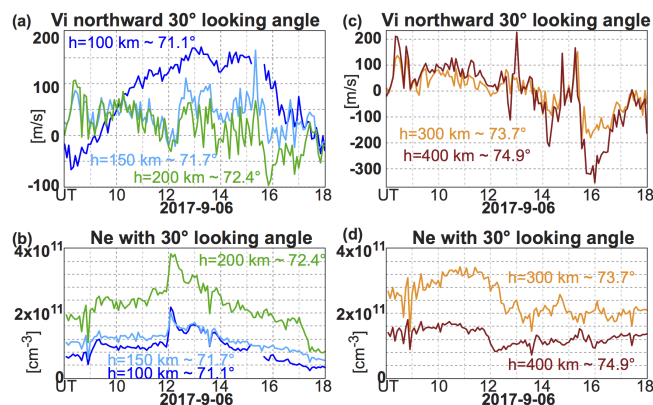
Figure 5. Ionospheric electron density and ion velocity observed by EISCAT Tromsø VHF radar at from 69° GGlat (line-of site component when looking northward with 30° angle). Upper panels (a) and (c) show the ion velocity and lower panels (b) and (d) show the electron density.
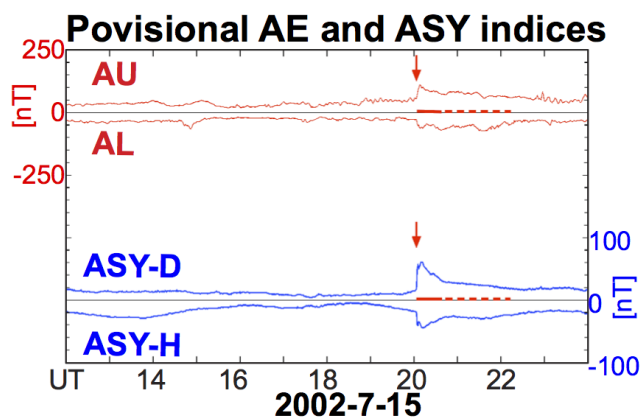
Figure 6. Web-interfaced quick-look plots of AE and ASY indices for 15 July, 2002. The red horizontal lines correspond to the period when the X-ray flux exceeds $3 \cdot 10^{-5}$ W/m^2, (>M3 class: solid lines) and 10^{-5} W/m^2, (>M class: dashed lines). The vertical red arrow denotes the start of the crochet.
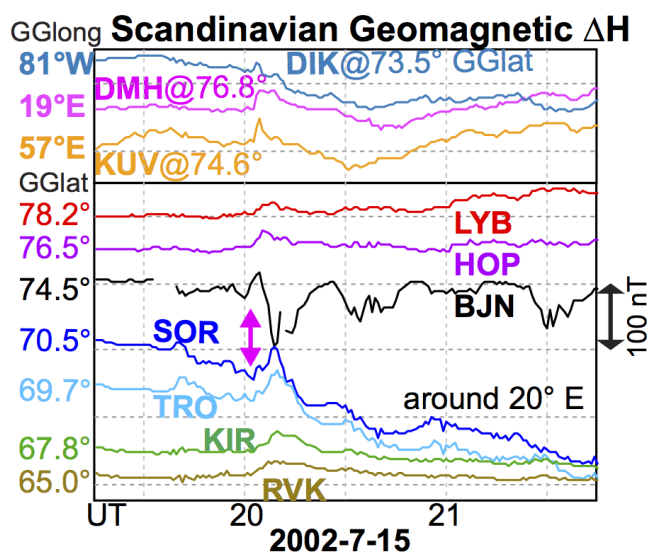
Figure 7. Geomagnetic ?H in northern Scandinavia and three other stations at around 75° GGlat (Stations at Figure 1 and Kullorsuaq: KUV) for the X3.0 flare on 15 July 2002. DIK, DMH, and KUV values are approximated by the change in local magnetic north direction. Red arrows denote the start of the X flare and subsolar crochet. At 20 UT, all stations are under sunlight at the ionosphere.
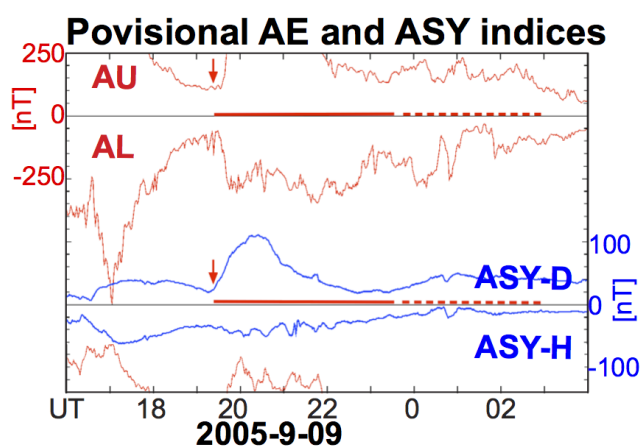
Figure 8. Same format as Figure 6 for 9 September 2005. A CME arrival and southward IMF turning at the Earth are at around 12:30 UT, and 19:30 UT, respectively.